

Article

Groundwater Contribution to Sewer Network Baseflow in an Urban Catchment-Case Study of Pin Sec Catchment, Nantes, France

Fabrice Rodriguez ^{1,2,*} , Amélie-Laure Le Delliou ^{1,3}, Hervé Andrieu ^{1,2} and Jorge Gironás ^{4,5,6,7} 

¹ Gers Laboratoire Eau et Environnement, Université Gustave Eiffel, Ifsttar, 44343 Bouguenais, France; al.le.delliou@groupeginger.com (A.-L.L.D.); andrieuherve@orange.fr (H.A.)

² Irstv Fr Cnrs 2488, rue de la Noé, 44321 Nantes, France

³ Ginger Burgeap Nantes, 44806 St Herblain, France

⁴ Departamento de Ingeniería Hidráulica y Ambiental, Pontificia Universidad Católica de Chile, Santiago 7820436, Chile; jgironas@ing.puc.cl

⁵ Centro de Investigación para la Gestión Integrada de Riesgo de Desastres Anid/Fondap/15110017, Santiago 7820436, Chile

⁶ Centro de Desarrollo Urbano Sustentable Anid/Fondap/15110020, Santiago 7530092, Chile

⁷ Centro Interdisciplinario de Cambio Global, Pontificia Universidad Católica de Chile, Santiago 7820436, Chile

* Correspondence: fabrice.rodriguez@ifsttar.fr; Tel.: +33-(0)24084588

Received: 21 December 2019; Accepted: 21 February 2020; Published: 3 March 2020



Abstract: Sewer systems affect urban soil characteristics and subsoil water flow. The direct connection observed between baseflow in sewer systems under drainage infiltrations and piezometric levels influences the hydrological behavior of urban catchments, and must consequently be considered in the hydrologic modeling of urban areas. This research studies the groundwater contribution to sewer networks by first characterizing the phenomenon using experimental data recorded on a small urban catchment in Nantes (France). Then, the model MODFLOW was used to simulate the infiltration of groundwater into a sewer network and model dry weather flows at an urban catchment scale. This application of MODFLOW requires representing, in a simplified way, the interactions between the soil and the sewer trench, which acts as a drain. Observed average groundwater levels were satisfactorily simulated by the model while the baseflow dynamics is well reproduced. Nonetheless, soil parameters resulted to be very sensitive, and achieving good results for joint groundwater levels and baseflow was not possible.

Keywords: groundwater; urban hydrology; drainage; modeling; sewer; baseflow

1. Introduction

Urbanization modifies land use and affects soil, sub-soil and subsurface processes in different ways. Urban features as well as surface and underground infrastructure can have a strong impact on groundwater levels. Some causes explaining a reduction in groundwater include an infiltration decrease due to additional imperviousness, groundwater pumping for various urban water uses, and groundwater flow into drainage trenches [1]. On the other hand, leakage from water supply and waste water networks becomes a source of recharge for urban groundwater [2–5]. Furthermore, leakage from waste water systems is also a possible source of groundwater contamination [6]. Despite aquifer levels and stream flow having proved to be related in various rural contexts [7,8], few studies have focused on examining this relationship in urban catchments [5,9–11]. Soil water infiltration in

sewers, however, is a phenomenon affecting urban hydrology, sewerage and waste water treatment plant management [12,13]. Initially, the presence of soil water in wastewater sewerage was revealed by [14,15], when flow variations in separate wastewater sewerage during wet weather periods were commonly attributed to inappropriate or irregular stormwater runoff connections. These authors showed that groundwater seep into the sewers through defective cracks once the water table level reaches the depth at which sewers are buried. This phenomenon has been recently reinforced by [13] for several Flemish catchments; some interesting stable isotopes methods have been used to detect and estimate groundwater intrusions in sewers in Nancy, France [16] and in Brussels, Belgium [17] and temperature-based methods in Trondheim, Norway [18]. Similarly, [9] showed that soil water may explain the variations of runoff coefficients observed on a small urban catchment in the city of Nantes, France, as groundwater drainage flow becomes significant once the water table exceeds a given threshold. The flowrate in sewers is the sum of runoff during rain events, wastewaters from housing (for separate wastewater or combined sewers), and a groundwater infiltration component, representing the baseflow in sewers; this component is often part of “extraneous” water in sewers. Interestingly, [19] suggest the appropriate terminology of urban “karst” to denote the multiple water soil and pipe interactions below the surface. Despite the relevance of improving our understanding of the impact of groundwater drained by urban sewer systems, only a few efforts are currently devoted to the problem. Groundwater drainage by sewers is often noted in literature [20], although is rarely quantified when assessing the urban water budget. Only a few papers deal with the determination of the urban water budget, likely due to the lack of reliable data of all the water budget components (i.e., rainfall, evapotranspiration, surface and groundwater flow rates). This lack of knowledge must be addressed as urban stormwater practices increasingly consider innovative infiltration-based technologies and approaches to mitigate the hydrological impacts of urbanization [21]. Thus, a better understanding and quantification of the fate of urban soil water becomes essential [22,23].

The first attempts to represent the interaction between surface water and the aquifer in urban integrated hydrological models were simple and conceptual. Aquacycle [24] and the Storm Water Management Model (SWMM, [25]) are examples of such models. In a comprehensive review of ten stormwater models, [26] identified the models able to simulate the groundwater baseflow component, mostly through a conceptual linear reservoir. Some of the more recent physically-based modeling efforts consider soil drainage by sewers. An integrated sewer-aquifer model was developed [27] to test the effects of future buried drains on both groundwater flow and sewer infiltration phenomena. This integration proved to be relevant to describe the groundwater-sewer interactions. The Network Exfiltration and Infiltration Model (NEIMO) model [28] was developed in close connection with already available groundwater models such as MODFLOW [29] or FEFLOW [30], to simulate infiltration and exfiltration processes. This modeling approach requires developing an integrated modeling framework like Urban Volume and Quality (UVQ) developed by CSIRO, Australia [31,32]. MODFLOW was used [33] to analyze the relevant infiltration parameters at a local scale, and compared a 1D-infiltration approach and a MODFLOW modeling approach to model groundwater infiltration at a larger scale. Overall, coupling groundwater models with the simulation of infiltration/exfiltration processes is a major challenge, especially due to the high uncertainty associated with these models [34]. The coupling of a hydraulic model was realized by [35] with both a groundwater model and a sewer failure estimation approach to identify the sections potentially affected by infiltration in coastal urban areas. Satisfying results were obtained by [11] with regard to the groundwater infiltration by coupling two commercial models MIKE URBAN for simulation of sewer flow and MIKE SHE for simulation of groundwater transport. The Urban Runoff Branching Structure Model (URBS-MO) [36] was developed to represent surface and subsurface water flows while focusing on the impact of sewer networks. Although the model simulates groundwater drainage by sewer, real observations at a local scale to test this component of the model were not available. Finally, [5] coupled the hydrological/water management WEAP model and MODFLOW to verify a strong stream-aquifer interaction in areas with shallow groundwater, as well as quantify the local recharge associated with pipe leaks and

inefficient urban irrigation. Overall, the literature review shows that much more experimental data and modeling using comprehensive 3D modeling tools such as MODFLOW, are needed to better understand and quantify the impact of groundwater infiltration and groundwater levels on low flows in urban environments.

This study investigates the interactions between urban groundwater and baseflow in wastewater and stormwater sewer systems, and its first goal is to better understand their role on the hydrological budget of an urban catchment. These interactions are analyzed and quantified using a field study conducted in the “Pin Sec” catchment, located in the city of Nantes (France) [37]. The second objective consists of testing the ability of a groundwater modeling tool to mimic these interactions. The results are used to build a numerical model focused on simulating the hydrological behavior of the urban soil and low flows in the sewer system. The outline of this paper is as follows: the next section presents the case study and the methods adopted in this work, which focus on using MODFLOW to model baseflow and interactions between the sewer systems and groundwater at catchment scale. The results section presents and compares observed and simulated groundwater levels and baseflow discharges. Finally, the last section summarizes our results and highlights the main conclusions.

2. Materials and Methods

2.1. *In-Situ Interactions Between Baseflow and Groundwater Levels*

2.1.1. Case Study

The experimental area is part of the Observatoire Nantais des Environnements Urbains (ONEVU) initiative, devoted to long-term monitoring of water and pollutant fluxes and soil-atmosphere exchanges in urban settings [37]. The Pin Sec catchment is located in the East of Nantes (France) between the Loire and the Erdre rivers. The area is under an oceanic climate, with frequent but not very intense rainfalls. The Pin Sec neighborhood developed between 1930 and 1970 is mainly composed of single and multi-family housing (Figure 1). This 31 ha catchment (called urban catchment) belongs to a larger hydrogeological catchment of 120 ha, both of them are represented on Figure 1. This catchment has a gentle slope, the highest altitude of the catchment is 28 m asl and the lowest is 13 m. The Pin sec catchment has an imperviousness of 45% and is equipped with a 50 years old separate sewer network. The wastewater and stormwater sewer systems have total lengths of 7.3 and 4 km, and mean depths of 2 and 2.9 m respectively. Although the wastewater sewer network is denser than the stormwater system, both are mainly superimposed, and both present cracks or faulty sealing joints. Both system outlets, while collecting water from the same geographic area, are not located in the same place. The stormwater system is connected to the Gohards river, whereas the wastewater sewer system drains into a downstream combined sewer system. Gohards river stream is an old river which was buried between 1945 and 2012 and which has been re-opened through a renovation urban planning of this area in 2012. It is a perennial stream.

Recorded data include (1) 5 min rainfall records from 1999 to 2010, deduced from the average of 3 rain gauges covering the study area, (2) 5-min flow discharge records at the outlet of both the stormwater and the wastewater systems from 1 September 2006 to 31 August 2008, (3) 20-min groundwater levels measured with pressure sensors in eleven piezometers located throughout the catchment from 1 September 2006 to 31 August 2008 (one piezometer, PZGN being only used to map the groundwater level contours), and (4) other meteorological records as well as evapotranspiration estimated with the Penman method, measured 12 km away from the catchment outlet, from 1999 to 2010. We focus our analysis on the main period between 1 September 2006 and 31 August 2008 (i.e., two hydrological years), but we also used year 2002 for some modeling tests as rainfall characteristics were representative of the average conditions in the area.

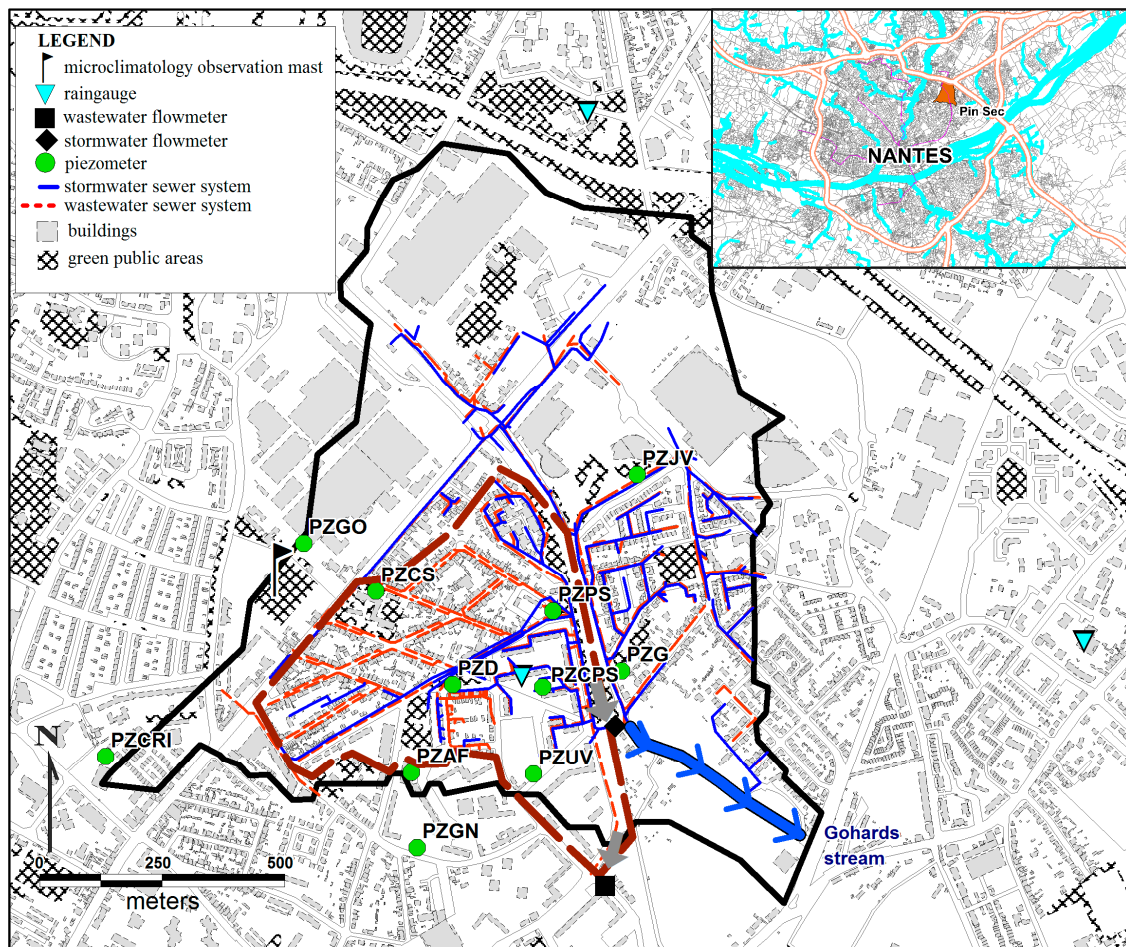


Figure 1. Pin Sec catchment within the Observatoire Nantais des Environnements Urbains (ONEVU) territory and location of the piezometers (green circles). The dotted brown and continuous black lines represent the boundary of the urban catchment and the hydrogeological catchment respectively. The large arrows represent the main sewer flow directions. By convention, north is placed at the top of the following maps. PZPS is located $47^{\circ}14'43.0''$ N $1^{\circ}31'09.1''$ W.

2.1.2. Geology and Hydrogeology

The city of Nantes has developed on the Armorican massif, and especially in the south Armorican shear zone. The geology is mainly composed of a mica-schists bedrock and a stack of alluvial deposits along the Loire River. On the Pin sec catchment, the mica-schists bedrock is covered with altered mica-schists, silty eolian deposits and alluvial deposits along the Gohards stream (Figure 2a) [38,39]. The piezometers are mainly located in the top layers and especially within altered mica-schists, with a drilling depth varying from 4 to 8 m (Figure 2b); for two of them, the depth was limited due to hard non altered micaschists. The hydraulic conductivities estimated from in-situ measurements by water bail tests [40] using the Hvorslev method [41] varies from $8.5 \cdot 10^{-8}$ to $1.8 \cdot 10^{-5} \text{ m s}^{-1}$ [42]. Piezometer PZGN is out of the hydrogeological catchment and was not considered for further results. From now on groundwater level will designate the level of the saturated zone, which is equivalent to the local groundwater level in our case study.

The piezometers were used for mapping the behavior of the water table on the catchment. Groundwater level contours were interpolated using inverse distance weighting (IDW) techniques with Vertical Mapper© in Mapinfo platform, and used to determine groundwater main flow directions. The groundwater levels of the high water table periods are presented in Figure 3. Note that the upstream condition of the water table is given by two piezometers (PZCRI and PZGO) located at the upper limit

of the catchment, and that groundwater moves in the northwest-southeast direction towards the stream outlet following the surface slope. The low water table condition is characterized by a similar profile.

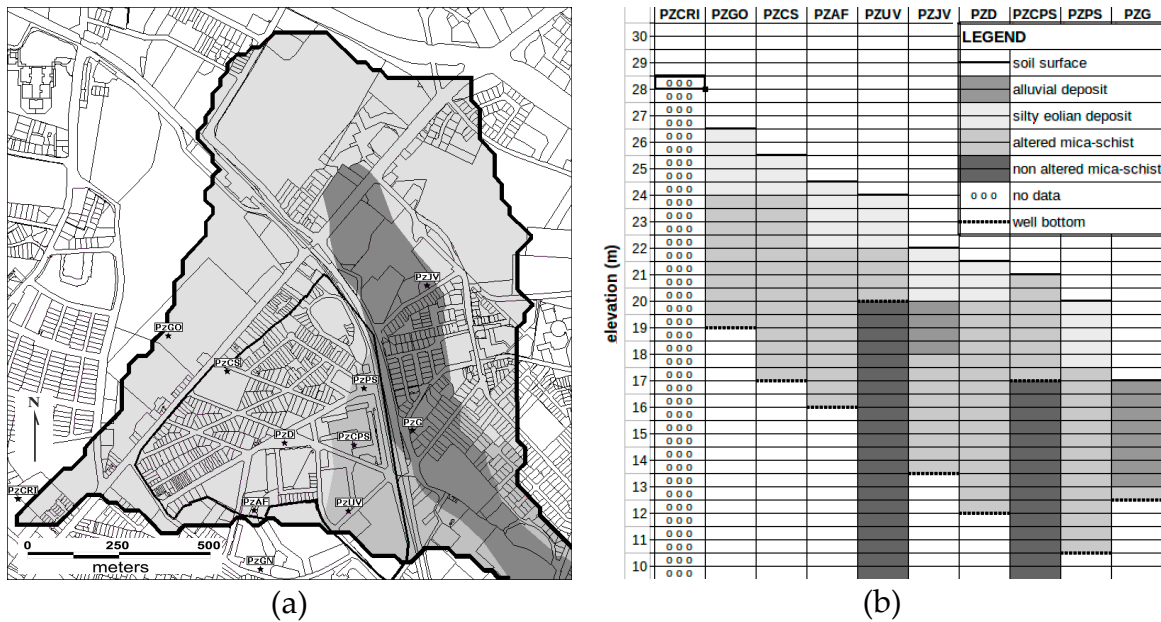


Figure 2. (a) Main geological layers on the Pin sec catchment: (non-altered micaschists are not visible because below the other layers); (b) Soil profiles of the set of monitored piezometers, ordered from upstream to downstream. Colors representing the geological layers on (a) refer to the Legend in (b).

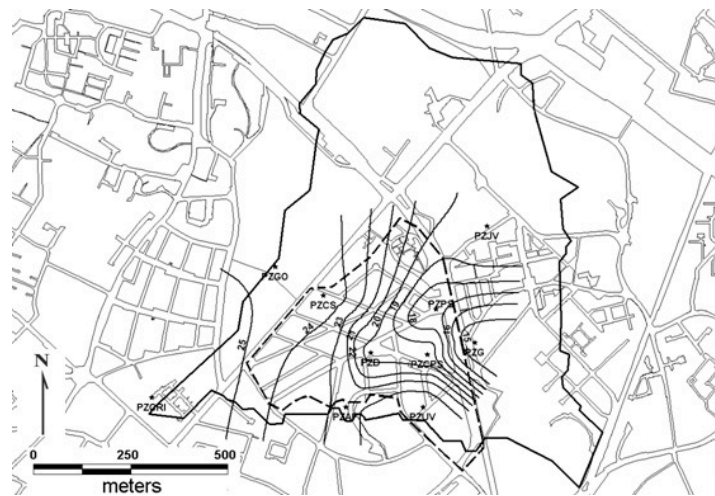


Figure 3. Groundwater level contours (hydraulic heads in m) deduced from the piezometric data interpolation on 7th March, 2007.

2.1.3. Baseflow in Sewer Networks

Both waste- and stormwater systems outlets are equipped with continuous flow rate measurement devices that use triangular weirs. Nonetheless, measuring the lowest flow rates within sewers has proved difficult as dry-weather flows do not necessarily reach the minimum water depth (~3 cm) needed for proper velocity measurement. Diurnal patterns of the wastewater flow rates show a typical domestic double-bump flow during dry weather time (Figure 4), and an increase of this flow during rain weather, due to parasitic waters (due to both wrong sewer connexions and groundwater infiltration). The stormwater flow rate is typical for urban catchments, with a fast hydrological response related to the runoff produced by impervious areas. In this study, baseflow is considered on a daily basis.

Stormwater baseflow is basically the minimum flowrate of each day. Because of the small size of the catchment, minimum wastewater flows corresponding to water draining from the water table are assumed to occur in the middle of the night [43–45]. Thus, we assume that the flow rate at 4:00 A.M. is representative of this drainage flow. Those days in which rain takes place are removed from the wastewater and stormwater discharge records to assess baseflow at the outlet of both systems during the study period (i.e., 65% of the time).

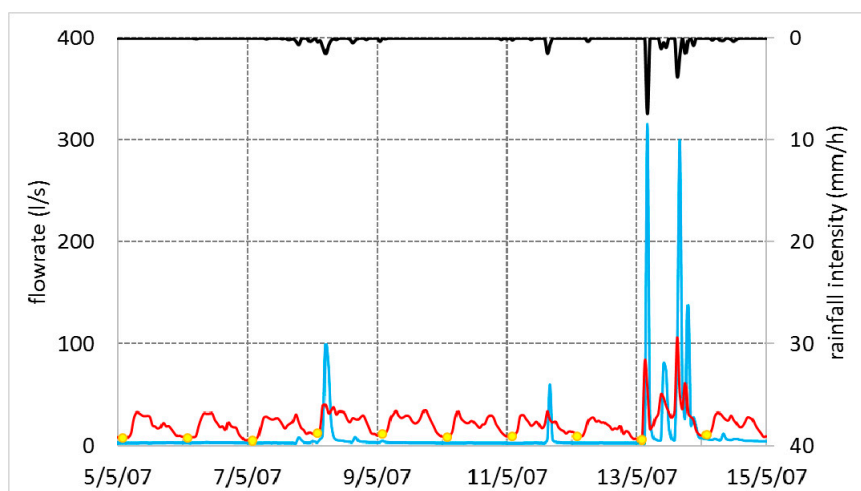


Figure 4. Dynamics of flowrates in both sewers (wastewater in red and stormwater in blue) during 10 days in May, 2007. The yellow dots show the minimum nighttime wastewater flow, used for the daily baseflow estimation.

2.2. Groundwater Modeling at the Urban Catchment Scale

Our aim in proposing a model to represent soil-sewer interactions is to improve our understanding of water fluxes in urban catchments. We use the groundwater model MODFLOW [29] to simulate these interactions because of (1) its widely-used extensive modeling capabilities [46], (2) its drainage modeling options to account for soil discontinuities using fine discretizations, and (3) the possibility of easily linking MODFLOW with other models. Few studies, however, have used the model in urban groundwater modeling [5,33,47–49], and in doing so, quite large grid resolutions (100–500 m) are adopted. In our study MODFLOW is used at a much finer resolution to represent sewers or buried trenches and their discontinuities in detail. Simple application conditions have been retained, because the use of MODFLOW in an urban context is not frequent and a cautious approach has been adopted. Moreover, the urban soil is both vertical and horizontal heterogeneous, and therefore not well documented.

2.2.1. Main Modeling Principles and Assumptions

MODFLOW uses a finite-difference approximation and an implicit scheme [29] to solve the 3D groundwater flow diffusion equation. In our implementation, the geological features of the catchment are deduced from the geological characteristics found in the case study (i.e., silt, altered and non-altered mica-schist). Two soil layers are defined from base to top: (1) a basement layer consisting of non-altered mica-schists; (2) a topsoil layer consisting of silty eolian deposits and altered mica-schists on the main part of the area, and alluvial deposits on the downstream part; this topsoil layer contains the sewer trenches.

Three MODFLOW modeling options were tested to represent the sewer trench, as this element cannot be explicitly implemented in the model: (1) a basic modification of the hydrodynamic properties of the cells containing the trench; (2) a field trench parallel to the surface slope with a small drainage

capacity, using the drain package (DRAIN); and (3) a representation of the sewer network using a river with the river package (RIV).

A preliminary sensitivity analysis was carried out at a street scale for a 100×100 m unit element, both in steady state and transient conditions (not presented here). This analysis helped to understand the impact of the modeling configurations (grid resolution and the sewer trench representation option) on both groundwater levels and flows simulation. Moreover, the influence of the main parameters used in the model (i.e., sewer trench conductance, hydraulic conductivities, specific yield and specific storage) was analyzed. The choices about the parameters or configurations described below were not adopted to replicate experimental results, but to retain realistic characteristics of the subsurface processes to be represented.

The grid resolution in our analysis varied between 1 and 10 m and affected mainly the water flows. Finally, a 4 m grid cell resolution was chosen. This size is quite large to represent the sewer trenches encompassing sewer pipes, but is a good compromise given the area of the study catchment (120 ha). Along the three tested options, the option using the DRAIN package to represent the sewer trench proved best to represent the saturated zone drainage by a sewer, because it can better reproduce the decreasing groundwater near the trench. Specific yields and conductivities are the main sensitive parameters, influencing both the groundwater levels and the flows. Due to the low impact of anisotropy in our sensitivity analysis, conductivities are considered homogenous in the three directions. The water flux increases with the hydraulic conductivities, while the groundwater level decreases. The initial hydraulic conductivities are estimated from in-situ measurements described above (§2.1.2). The influence of the specific yield of the topsoil layer is significant for the sewer trench outflow: the downstream flow reduces by 7% when specific yield decreases from 20% to 5%, which are typical values assessed by [50].

The field drainage system representing the sewer trench is characterized by a drain hydraulic conductance (L^2/T) (conductance thereafter), which depends a priori on the material and characteristics of the drain. Since the conductance is usually unknown, it must be estimated by calibration [49,51]. We first assessed the range of variation of the conductance from the sewer baseflow observations. As discussed by [51], the discharge rate to drain cells may be calculated as the product of the conductance and the head gradient ($h-d$), where h is the hydraulic head and d is the elevation of the drain. We integrated this relation at the whole sewer network scale, which allows estimating a global conductance associated with the total groundwater flowrate in sewers. Assuming that the baseflow in sewers is only due to groundwater infiltrations, the application of this relation for the high water level period during year 2007 and for the total length of flooded sewer pipes generates a conductance of ~ 0.9 m²/day. This parameter only changes the water flows and its effect on groundwater levels is less significant. In the end, the specific storage slightly affects the modeling results, as it ranges theoretically from 3.3×10^{-6} m⁻¹ (rock) to 2×10^2 m⁻¹ (plastic clay) [51]. A medium value of 1×10^{-5} m⁻¹ was adopted initially.

2.2.2. Urban Groundwater Modeling at the Catchment Scale and Application to the Case Study

The MODFLOW model is used on the Pin Sec catchment to assess soil water-sewer interactions at the urban catchment scale. Furthermore, certain simplifications not considered in the sensitivity analysis for the unit element were adopted. The two soil layers are represented in this way: (1) the basement layer is located in the entire catchment at a mean depth of 18 m, and (2) the topsoil layer is located in the valley area around the old stream bed, with a mean depth of 2 m. Because both the stormwater and wastewater systems are often placed within the same trench below the street surface, both networks have been combined to represent the draining trench in the soil. Thus, the field drain represents both stormwater and wastewater networks.

Boundary conditions are stipulated as follows and summarized on Figure 5: (1) a zero-flux condition is defined in the upstream boundary of the hydrogeological catchment by considering no-flow cells and (2) a river boundary condition representing the Gohards stream is defined as the

downstream condition by using the River package (RIV) on a 200 m long stream; it is a head-dependant boundary condition. The combined 'field drain', representing the sewer systems, drains into this stream. A one hydrological year simulation in transient conditions is performed on the catchment using a daily time step. The transient simulation is initialized using the steady state case calibrated to the field data observed the first day of simulation. The recharge is calculated on a daily basis using the urban surface hydrological model URBS-MO, already successfully applied to urban catchments in the area to simulate the various components of the water budget [36]. The recharge is assumed to be uniform throughout the catchment, and equal to the infiltration calculated by URBS-MO (i.e., rainfall intensity minus both the actual evapotranspiration and surface runoff). Rainfall and potential evapotranspiration data available for the Pin Sec catchment were used with URBS-MO. The initial set of parameters for the simulation is deduced from the observations and a first steady state simulation conducted on the catchment (Table 1). Specific yield and specific storage values are the same as those used for the sensitivity analysis; they vary in space along with the two geological layers defined in this catchment. Due to the lack of information about the spatial distribution of cracks and faulty sealing joints in sewers and to an homogeneous age of the pipes, the drain conductance is assumed to be uniform and the initial value is deduced from the groundwater baseflow observed in the catchment sewers presented in next section.

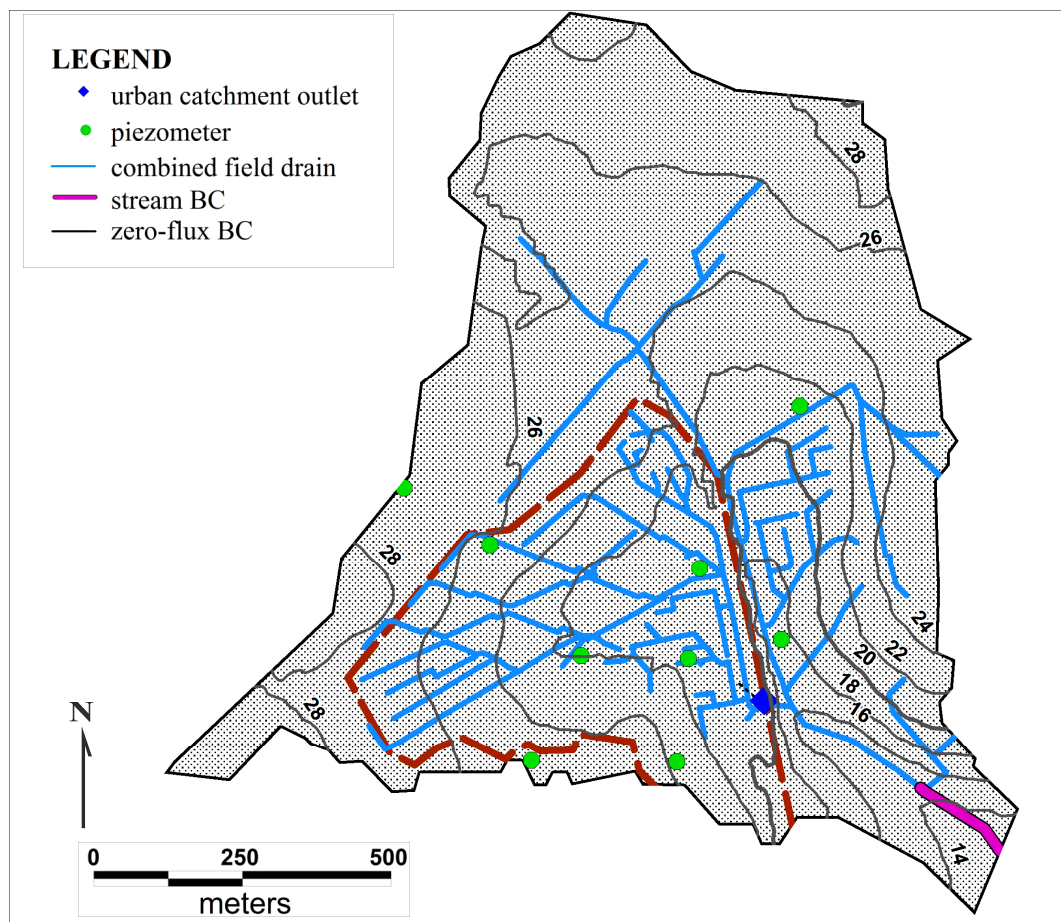


Figure 5. Main boundary conditions applied to the catchment scale model. The 4×4 m grid is not perceptible at this scale; the relief is represented with gray elevation contours (altitude asl in m).

The model simulates (1) the hydraulic head and groundwater flux at any grid cell of the domain, and (2) the drain flux at any point of the field drain system. Special attention is paid to the hydraulic head at field piezometers and the flow at the outlet of the catchment, where a flow gauge is located

(Figure 1). The period going from September 2006 to September 2007 is used for calibration, while the period between September 2007 and September 2008 is used for validation.

Table 1. Parameters used within the catchment modelling for the different layers.

Parameter	Loess and Altered Mica-Schists	Mica-Schists	Alluvial Deposits
Initial values			
Hydraulic conductivity (m/s)	1×10^{-6}	1×10^{-7}	1×10^{-6}
Specific yield (%)	20	20	20
Specific storage (1/m)	1×10^{-5}	1×10^{-5}	1×10^{-5}
Drain conductance (m^2/day)	-	0.9	-
Calibrated values			
Hydraulic conductivity (m/s)	1×10^{-4}	1×10^{-6}	1×10^{-3}
Specific yield (%)	5	10	10
Specific storage (1/m)	1×10^{-2}	5×10^{-4}	1×10^{-2}
Drain conductance (m^2/day)	-	5	-

3. Results

3.1. Groundwater Dynamics and Experimental Relationship Between Groundwater Level and Baseflow

The temporal dynamics of groundwater levels are presented in Figure 6 for two of the piezometers; more details may be found in [39]. The mean difference between the high and low water table was approximately 1.7 m during the period 2006–2007, and 1.5 m during the period 2007–2008. This difference varied from ~3 m upstream to 1 m downstream (Table 2).

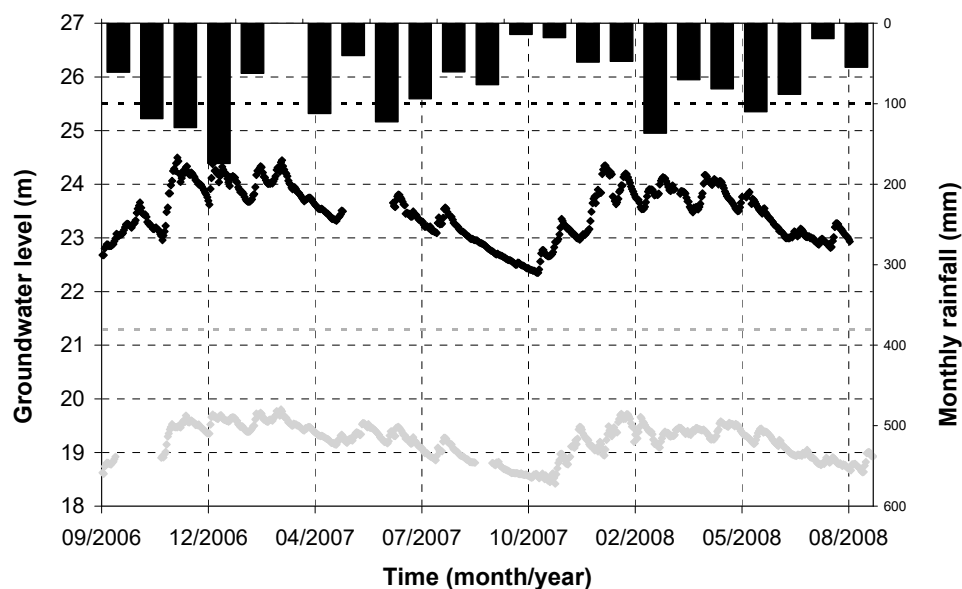


Figure 6. Daily dynamics of the groundwater levels in piezometer PZCS (black) and PZD (grey) from 2006 to 2008 on the Pin Sec catchment. The corresponding surface elevations are plotted with black and grey dotted lines. Bars correspond to monthly rainfall.

Groundwater infiltration in sewer networks depended on several factors such as the location and shape of the water table, the depth of the sewers, and their conditions (e.g., presence of defects). [9] collected information in a small urban catchment in the metropolitan area where the Pin Sec catchment is located, and noticed that groundwater drainage flow became significant once the

water table reached a depth of 1.5 m below the surface, and increased as the water table rose. In fact, the mean sewer depth in the area is ~1.2 m below the surface.

Table 2. Main features of the groundwater levels during the studied period (September, 2006 to September 2008). The piezometers are presented from upstream (left) to downstream (right). Z_{soil} is the altitude of the corresponding piezometer; ‘gw depth’ is the groundwater depth from the surface level; $R^2(SW)$ and $R^2(WW)$ are the determination coefficient of the polynomial regression relationship for stormwater and wastewater baseflow, respectively (2006–2007 period) (See Figure 7 for piezometer PZPS).

	PZCRI	PZGO	PZCS	PZAF	PZUV	PZJV	PZD	PZCPS	PZPS	PZG
Z_{soil} (m)	28.70	26.70	25.50	24.50	23.80	22.14	21.30	21.05	20.00	17.20
Average gw depth (m)	4.14	2.73	2.04	2.24	1.82	2.77	2.09	2.17	3.35	3.35
Minimum gw depth (m)	5.18	4.14	3.16	3.01	3.60	3.52	2.94	2.75	3.72	4.01
Maximum gw depth(m)	2.85	1.65	1.00	1.53	0.10	0.13	1.48	1.66	2.76	2.73
$R^2(SW)$	0.380	0.649	0.640	0.533	0.711	0.609	0.713	0.729	0.817	0.660
$R^2(WW)$	0.250	0.766	0.828	0.646	0.753	0.729	0.802	0.762	0.822	0.640

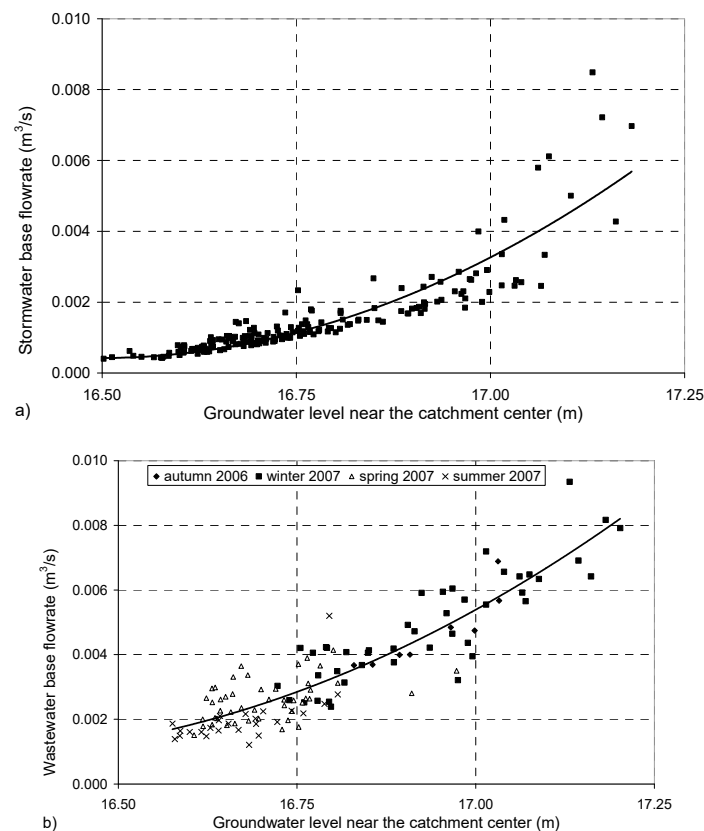


Figure 7. Relationship between daily groundwater drainage flow Q in (a) stormwater and (b) wastewater sewers, and the groundwater level H for the 2006–2007 period. The groundwater level is observed on piezometer PZPS, located on the main sewer intersection. Polynomial regression relationships are $y = 0.0112x^2 - 0.3693x + 3.0460$ ($R^2(SW) = 0.817$) for (a) stormwater and $y = 0.0083x^2 - 0.2711x + 2.2056$ ($R^2(WW) = 0.822$) for (b) wastewater.

The connection between the average groundwater level of the catchment H and daily baseflow Q in the sewer systems is evident from Figure 7. A specific piezometer (PZPS) located near the main sewer intersection and representative of the average behaviour of the groundwater level dynamics has been chosen; it is considered to be in the catchment center according to groundwater main flow directions. Figure 7a shows a $Q \sim H^2$ relationship for the baseflow in the storm sewer, which is typical of ideal field drains used in rural hydrology [52]. Groundwater drainage is observed at the outlet of the stormwater

network during the entire observation period, which demonstrates that sewer infiltrations take place all year round. The behavior is similar for the wastewater sewers (Figure 7b). The wastewater baseflow barely varies during summer when the water table is low (between July and October). Baseflow becomes substantial again when the groundwater level for this piezometer PZPS exceeds a threshold value of ~ 16.75 m (i.e., 3.2 m below the surface). Waste- and storm-baseflows differ because the drainage density of the wastewater system is higher than that of the stormwater system. This is the reason why the $Q \sim H^2$ relationships are more consistent for the wastewater baseflow than the stormwater baseflow, as revealed by the determination coefficient variation $R^2(\text{SW})$ or $R^2(\text{WW})$ (Table 2). Additionally, these relationships are generally more pronounced for the downstream piezometers, closer to the baseflow monitoring locations.

This observation is confirmed by the map showing the sewer receiving groundwater contributions during the high water table period of 2007 (Figure 8). This map was realized through the superimposition of groundwater level contours (Figure 3) and the sewer depth levels deduced from GIS data. The total sewer length soaked during winter is 2.6 km for the wastewater sewers and 1.1 km for the stormwater sewers. Finally, the annual subsurface water volume drained into both sewer systems deduced from the sum of daily base-flows between September 2006 and August 2007 is 28% (wastewater sewer) and 14% (stormwater sewer) of the total rainfall respectively. This result proves that the base flow discharges in artificial sewer systems can be a major component of the urban water budget, as 42% of the total annual rainfall is drained to the sewer systems.

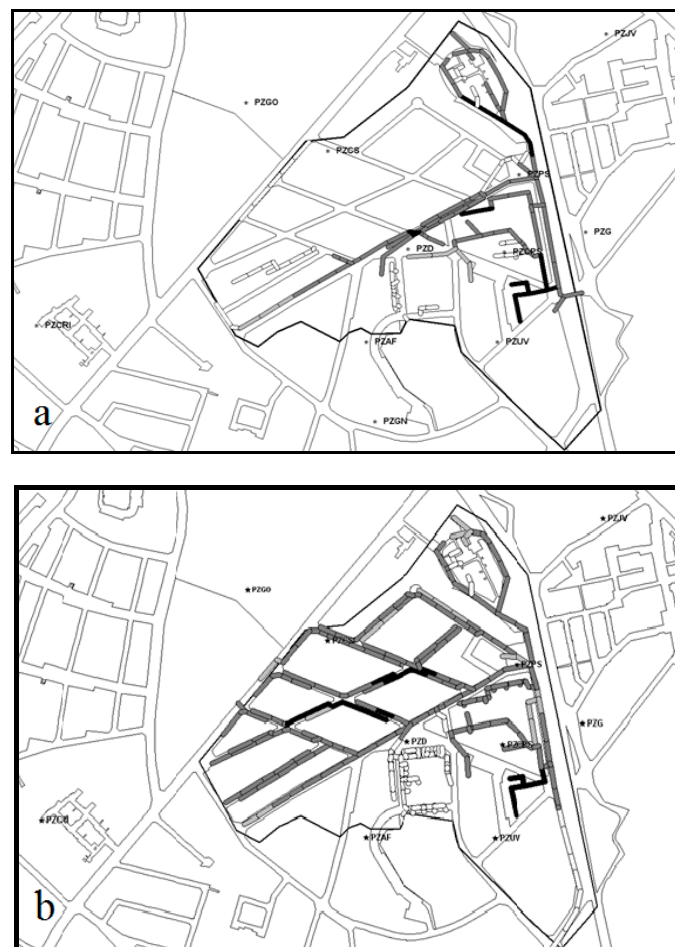


Figure 8. Sewer pipe network affected by groundwater during winter (2007/03/07): (a) stormwater network and (b) wastewater network. Black and light gray sewer pipes are located 1 m below and above the groundwater table respectively. Dark gray sewer pipes are between them.

3.2. Comparison between Modeling Results and Observed Data at the Catchment Scale

Three metrics were adopted for the evaluation of the model: the root mean square error (RMSE), a Bias error, and the determination coefficient R^2 :

$$RMSE = \sqrt{\frac{1}{n} \sum_{i=1}^n [V_2(t) - V_1(t)]^2} \quad (1)$$

$$Bias\ error = \frac{\sum_{i=1}^n V_2(t) - V_1(t)}{\sum_{i=1}^n V_1(t)} \quad (2)$$

$$R^2 = \frac{\left(\sum_{i=1}^n [V_2(t) - \bar{V}_2][V_2(t) - \bar{V}_1] \right)^2}{\sum_{i=1}^n (V_1(t) - \bar{V}_2)^2 \sum_{i=1}^n (V_1(t) - \bar{V}_1)^2} \quad (3)$$

where n is the number of time steps involved, V_1 and V_2 are the observed and simulated values, \bar{V}_1 and \bar{V}_2 the temporal average of V_1 and V_2 .

Absolute error (m) was used as well to estimate the difference between simulated and observed groundwater levels in specific piezometers.

3.2.1. Implementation and Calibration of MODFLOW at the Catchment Scale

In the MODFLOW model of the catchment, we first calibrated the hydraulic conductivity, specific yield and specific storage of each soil type by minimizing the global bias error between observed and simulated groundwater levels. Then we calibrated the drain conductance by maximizing the coefficient of determination R^2 between observed and simulated combined baseflows (i.e., stormwater + wastewater sewers baseflows) at the outlet of both sewer systems. The final calibration presented in Table 1 is achieved through a trial and error method. The obtained hydraulic conductivities are two orders of magnitude higher than the observed hydraulic conductivities using the piezometers. This result is consistent with previous statements following the application of other models to ditch-groundwater interactions [53], and confirms the difficulty to simulate groundwater flows and groundwater levels using a few specific point observations of the hydraulic conductivities. High soil heterogeneity, particularly in urban areas, cannot be well characterized using soil properties measurements sampled in a few locations, which leads to a poor simulation of the general groundwater behavior. Despite the differences between observed and calibrated conductivities, the observed differences between the different types of soil are consistent with the theory. Hence, the highest hydraulic conductivity is obtained for alluvial deposits, and the smallest one for mica-schist. Finally, the calibrated drain conductance is higher than initially estimated, which allows a better simulation of high values and the dynamics of the baseflow.

In order to assess the influence of the sewer system on the evolution of the groundwater levels, a complementary simulation of the catchment was done on the same period and with the same set of parameters by removing the sewer system and the corresponding field drain. This simulation exercise shows that the groundwater reaches the soil surface during the winter 2007–2008 on a significant part of the basin; that result clearly confirmed the importance of the drainage ensured by the sewer system [39].

3.2.2. Groundwater Level Distribution Assessment

The temporal and spatial simulation of groundwater levels is assessed using available piezometric records. Figure 9 illustrates the simulation of the isopiezometric contours for the high water table

period (7th March, 2007), and can be compared to the observed isopiezometric contours at the same date shown in Figure 3. At this period, the absolute errors between simulated and observed values may be larger than 2 m in some piezometers, especially on the south catchment boundary. They are however better in the middle of the catchment and near the outlet. In addition, absolute errors are higher around the piezometers distant from the sewer trenches. Note that the simulated contours in Figure 9 are plotted on a surface area larger than the experimental one, as the simulated catchment exceeds the piezometric set boundary. Consequently, the simulated flow directions differ significantly from observed ones near the urban catchment boundary, but are rather similar within the urban catchment. Nonetheless, at this time the simulated saturation level is often higher than the observed one. The simulated vs. observed groundwater level dynamics is assessed by computing the RMSE, bias error and R^2 for all the piezometer locations, both for the calibration and validation periods (Table 3). R^2 values are often smaller than 0.5 for the calibration stage, but increase for the validation stage. In general, the model underestimates the groundwater level for half of the piezometers (PZCPS, PZCS, PZGO, PZUV, PZJV) and overestimates it for the others. The boxplot analysis of the bias error (Figure 10) shows that the underestimation is mainly concentrated on the upstream part of the catchment (PZCRI, PZGO, PZCS, PZJV, PZUV), and might be explained by either the upstream boundary condition or the uniform recharge assumption. Indeed, the spatial analysis of the imperviousness coefficient of the Pin Sec catchment reveals that underestimated piezometric observations are located in more pervious areas within the catchment (i.e., green public parks). Hence, using a spatially distributed recharge could allow a more accurate modeling of the groundwater levels dynamics in these areas. Overall, the simulated groundwater levels compared properly with observed ones both for the calibration and validation periods (Figure 11), despite an underestimation of the model compared to the observed data at the beginning of the validation period, when a particularly dry autumn took place. In the absence of rain, the groundwater model simulates a groundwater level decrease higher than observed, which to some extent questions both the upstream boundary condition assumption and the recharge estimation. Moreover, the quite stable groundwater level observed during this period could be explained by a groundwater influx coming from upstream, which would disprove the assumed upstream boundary condition. Nonetheless, no observations outside the catchment are available to clarify this issue. Finally, drinking water leakage in the soil can occur, which would increase the recharge throughout the year and prevent the high decrease of groundwater levels observed in the simulation; this phenomenon has been discussed in several cities like Bucharest, Romania [4,49], St Louis, Missouri(US) [54] or Santiago, Chile [5].

Table 3. Metrics of simulated groundwater levels simulated in each piezometer for the calibration and validation stages. Data availability indicates the percentage of valid data available during the simulation period. Columns *in italics* denote piezometers with poor data availability.

Criterion	PZCRI	PZGO	PZCS	PZAF	PZUV	PZJV	PZD	PZCPS	PZPS	PZG
Calibration (2006–2007)										
Data availability (%)	100	96	87	96	100	100	88	94	100	96
R^2	0.66	0.32	0.48	0.50	0.44	0.48	0.24	0.36	0.45	0.44
Bias error (%)	6.87	−0.38	−3.47	3.36	−9.16	−3.12	7.02	−3.15	0.90	7.93
RMSE (m)	1.80	0.56	0.87	0.87	2.10	0.64	1.39	0.70	0.23	1.11
Validation (2007–2008)										
Data availability (%)	96	56	98	63	95	99	98	38	100	51
R^2	0.81	0.45	0.64	0.60	0.26	0.05	0.63	0.76	0.78	0.70
Bias Error (%)	−0.23	−3.68	−6.19	1.72	−2.07	−9.79	5.52	−3.07	3.72	5.45
RMSE (m)	0.61	0.40	1.42	0.31	4.91	1.78	1.03	0.28	0.58	0.55

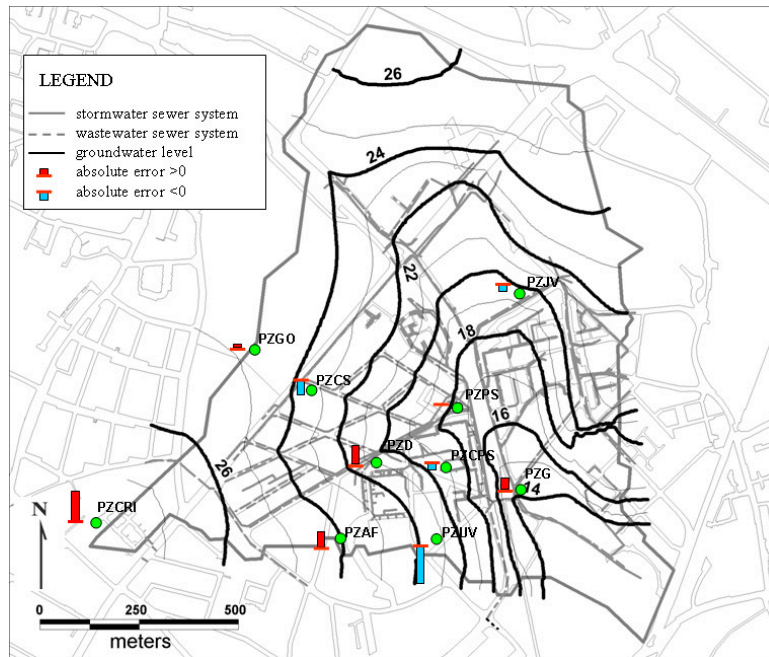


Figure 9. Groundwater level contours (hydraulic heads in m) simulated in transient state during the low groundwater table period (7th March, 2007) in the Pin Sec catchment. Absolute errors are represented by red and blue bars at each piezometer. Bar sizes show a variation from -2.66 m (PZUV) to 2.11 m (PZCRI).

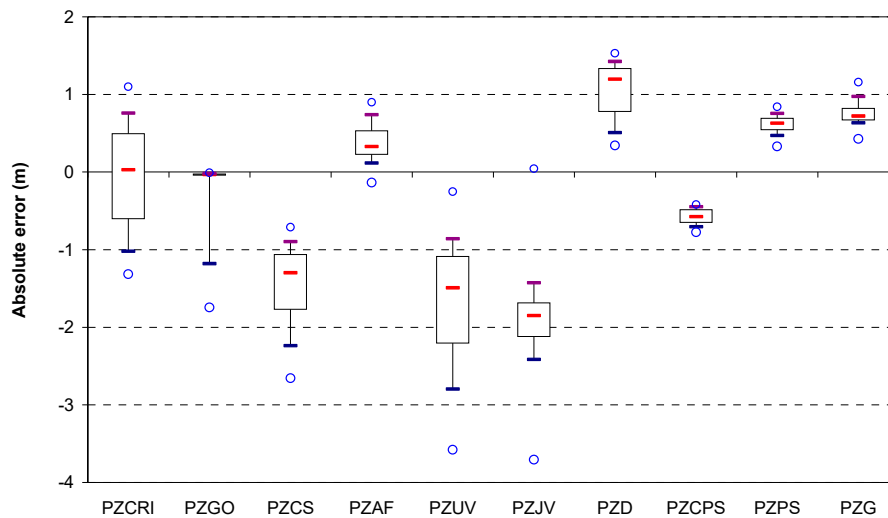


Figure 10. Box-plot characterizing the absolute error distribution between simulated and observed groundwater levels for the validation period (2007–2008). The piezometers are presented from upstream (left) to downstream (right). Small circles are minimum and maximum values red mark are the median, whereas the ends of the whiskers represent the 25th and 75th percentiles.

Figure 9 shows a small curvature of the simulated groundwater level contours near the sewer trenches caused by the local groundwater drawdown. Groundwater decrease is quite significant in places where sewer density is high (i.e., central and north portions of the catchment). This phenomenon is enhanced when the water table rises above the sewer system, and becomes less significant in summer. For simulated data samples, groundwater drawdown is higher during the wet year 2006–2007 with a decrease of about 0.3 m near the sewer trench, and a zone of influence ranging up to 120 m away from the trench axis.

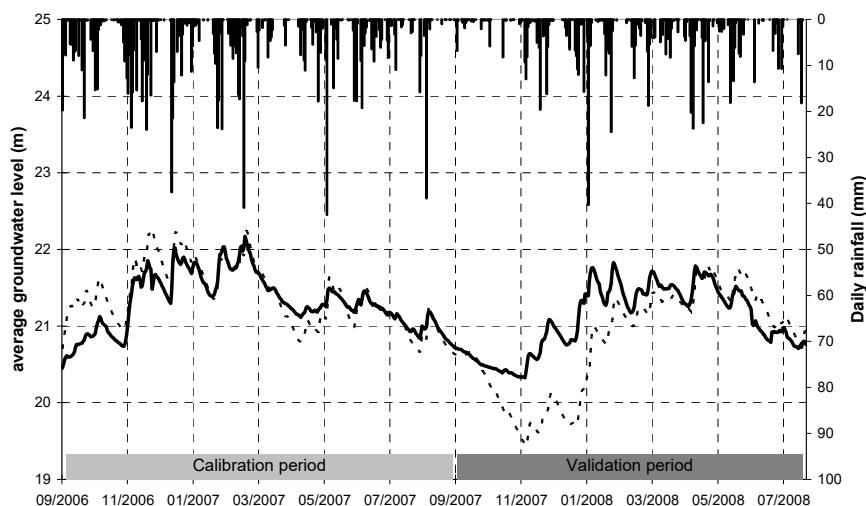


Figure 11. Comparison between simulated (dotted line) and observed (bold line) average hydraulic heads in the catchment from September 2006 to August 2008.

3.2.3. Baseflow Rate Assessment

The simulated soil water flux combines two components simulated in MODFLOW: groundwater flux within the soil and groundwater drainage inside the sewer trench. Both components flow in the same general direction forced by the catchment topography and the downstream condition imposed by the Gohards stream. Groundwater drainage may be compared with the baseflow discharge observed in both waste- and storm- sewer systems during the 2006–2007 simulation (note that the period 2007–2008 is not presented due to the lack of data). Figure 12 shows that the daily groundwater drainage component varies significantly, ranging from 50 m³/day during very dry periods (i.e., the end of summer 2007) to 2600 m³/day during the particularly humid 2006–2007 winter. Indeed, ~630 mm of rain (i.e., ~80% of the catchment mean annual rainfall) fell between November 2006 and April 2007 in the area. Unfortunately, a direct comparison between the simulated groundwater drainage flow and observed baseflow is difficult because of the lack of flow rate data. Considering the data actually available, the comparison focuses on the dynamic evolution of the baseflow. Simulated groundwater drainage and in-situ observations over the simulated period vary in a quite similar manner. Nonetheless the overestimation of the observed flows could not be reduced by further calibration, as drain conductance variations do not affect groundwater drainage significantly. As seen in the sensitivity analysis, soil hydraulic conductivities have more impact on the simulation than drain conductance. Because soil hydraulic conductivities affect not only groundwater drainage but also groundwater level, a simultaneous enhancement of both is not possible.

Special attention must be paid to the relationship between baseflow rates and groundwater levels. As discussed above and shown in Figure 7, both are strongly linked through a power-law function. Figure 13 overlaps simulated and observed values when considering the combined baseflow, and shows that the model can satisfactorily reproduce this groundwater level-baseflow relationship despite of the baseflow overestimation during high water table periods. Although only 32% of the experimental results during the 2006–2007 period are available simultaneously for both sewers, and apart from the low groundwater levels occurring in summer and discussed above, the validity of the relationship holds quite well.

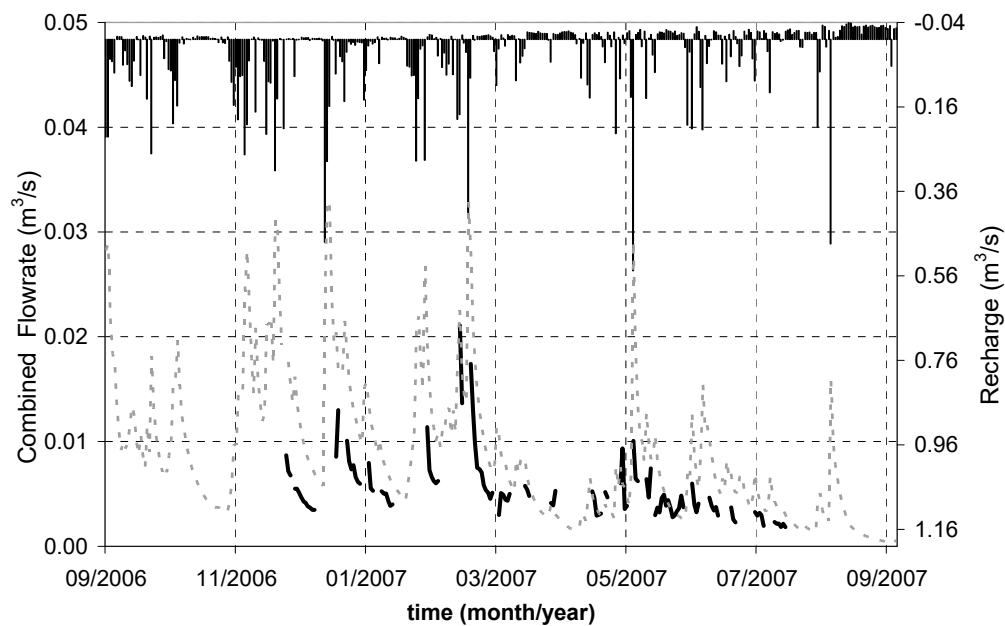


Figure 12. Comparison between simulated (dotted line) and observed (bold line) daily combined baseflow at the catchment outlet from September 2006 to September 2007. The recharge evolution shows the infiltration and evaporation periods during this simulation.

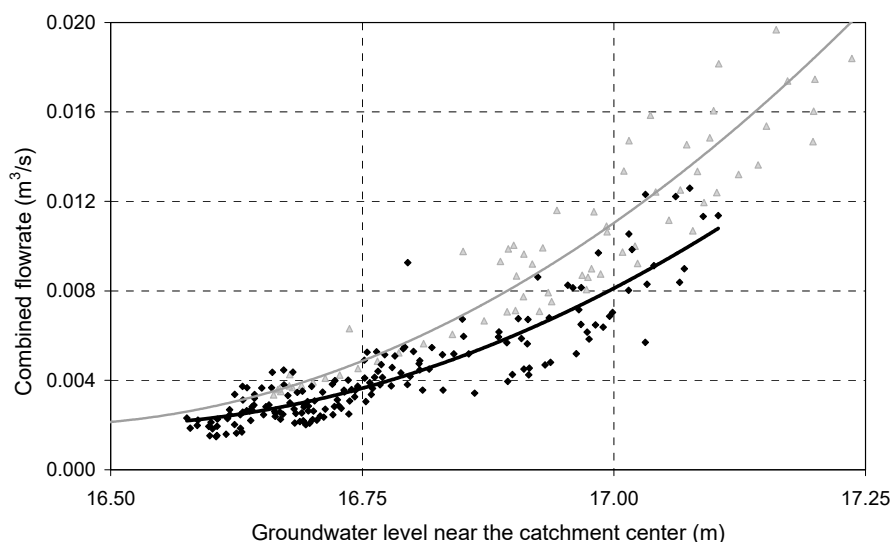


Figure 13. Combined daily baseflow in sewers vs. piezometric levels between September 2006 and September 2007. Both observed values (black points) and simulated values (grey points) are shown in the (0–0.02 m³/s) range of flowrates, along with their respective polynomial regression relationships: $y = 0.0225x^2 - 0.7404x + 6.1016$ ($R^2 = 0.803$) for the observed values and $y = 0.0276x^2 - 0.9060x + 7.4436$ ($R^2 = 0.908$) for the simulated values.

4. Conclusions

This study presents an experimental analysis and modeling of the interactions between groundwater and urban sewer systems in a 31 ha urban catchment located near Nantes, France. Groundwater contributions to flow in stormwater and wastewater systems due to sewers' defects were deduced from observed flow rates, whereas piezometric records were used to characterize the dynamics of groundwater levels in the catchment.

Overall, the experimental analysis reveals a strong co-fluctuation of groundwater levels and sewer baseflow, which is more pronounced in downstream piezometers. This study highlights

that two or three piezometers located near the catchment outlet are likely adequate to estimate the groundwater-baseflow relationship in an urban catchment. The total baseflow volume in wastewater sewers is larger than in stormwater sewers because of its larger coverage. On an annual basis, the total volume of soil water drained by both sewers is 42% of the total rainfall.

A MODFLOW model was implemented in the study catchment to simulate the groundwater dynamics and contribution to the sewer systems on a daily basis. This application proves the model ability to represent satisfactorily the spatial and temporal evolutions of groundwater levels, although low groundwater levels were underestimated. Spatial differences between modeled and observed groundwater levels in some locations could be explained by the spatial variability of the land uses and the urban soil configuration around each piezometer. The simulation of combined waste and storm water sewer baseflows is not entirely relevant because the model fails to reproduce the high values of baseflow. The calibration of the model lead to hydraulic conductivities values higher than those observed in the piezometers. In fact, the calibrated values are similar to those reported in the literature, and they are attributed to possible secondary porosities and hydraulic conductivity distributions comparable to those of a karstic system [55]. Hydraulic conductivity varies significantly in urban soils due to differences in their characteristics, the existence of different land-uses, and the presence of previous buried constructions.

More work is needed to improve our knowledge of urban soil water flow paths. Baseflow must be better measured, as flow meter sensors are not always reliable to be used with low flows. In addition, more observations at a local scale are needed to better understand groundwater-sewer interactions and improve large scale modeling efforts. Such data will come from either (1) physical models relying on better estimations of soil parameters, which can represent the influence area of a sewer trench, or (2) sensors located near the sewers. Groundwater models applied to urban catchments will require using a graded grid size with mesh refinements near sewers and more urbanized areas. Furthermore, better spatially distributed recharge estimations can also improve the performance of these models. This could be done by coupling the groundwater and surface water models, adopting better modeling frameworks like the modeling chain proposed by [56], or implementing other specific coupling modeling approaches. Finally, a better understanding of the occurrence and spatial distribution of leaks from drinking water pipes is also needed to improve the characterization of the recharge.

Author Contributions: This study was designed by F.R., A.-L.L.D., and H.A. The manuscript was prepared by F.R. and revised by H.A. and J.G. All authors have read and agreed to the published version of the manuscript.

Funding: This study received financial support from the French research programs ANR and INSU-EC2CO within the project Hy²ville, and from the Région Pays de la Loire. Funding from CONICYT/FONDAP grants 15110017 and 15110020 were also available.

Acknowledgments: We thank Nantes Métropole (Direction de la Géographie et de l'Observation) for providing the GIS data.

Conflicts of Interest: The authors declare no conflict of interest.

References

1. Lee, J.Y.; Choi, M.J.; Kim, Y.Y.; Lee, K.K. Evaluation of hydrologic data obtained from a local groundwater monitoring network in a metropolitan city, Korea. *Hydrol. Process.* **2005**, *19*, 2525–2537. [[CrossRef](#)]
2. Barrett, M.H.; Hiscock, K.M.; Pedley, S.; Lerner, D.N.; Tellam, J.H.; French, M.J. Marker species for identifying urban groundwater recharge sources: A review and case study in Nottingham, UK. *Water Res.* **1999**, *33*, 3083–3097. [[CrossRef](#)]
3. Lerner, D.N. Identifying and quantifying urban recharge: A review. *Hydrogeol. J.* **2002**, *10*, 134–152. [[CrossRef](#)]
4. Gogu, C.R.; Gaitanaru, D.; Boukhemacha, M.A.; Serpescu, I.; Litescu, L.; Zaharia, V.; Moldovan, A.; Mihailovici, M.J. Urban hydrogeology studies in Bucharest City, Romania. *Procedia Eng.* **2017**, *209*, 135–142. [[CrossRef](#)]

5. Sanzana, P.; Gironás, J.; Braud, I.; Muñoz, J.F.; Vicuña, S.; Reyes-Paecke, S.; de la Barrera, F.; Branger, F.; Rodriguez, F.; Vargas, X.; et al. Impact of Urban Growth and High Residential Irrigation on Streamflow and Groundwater Levels in a Peri-Urban Semiarid Catchment. *JAWRA J. Am. Water Resour. Assoc.* **2019**, *55*, 720–739. [[CrossRef](#)]
6. Reynolds, J.H.; Barrett, M.H. A review of the effects of sewer leakage on groundwater quality. *Water Environ. J.* **2003**, *17*, 34–39. [[CrossRef](#)]
7. Evans, M.G.; Burt, T.P.; Holden, J.; Adamson, J.K. Runoff generation and water table fluctuations in blanket peat: Evidence from UK data spanning the dry summer of 1995. *J. Hydrol.* **1999**, *221*, 141–160. [[CrossRef](#)]
8. Scibek, J.; Allen, D.M.; Cannon, A.J.; Whitfield, P.H. Groundwater–surface water interaction under scenarios of climate change using a high-resolution transient groundwater model. *J. Hydrol.* **2007**, *333*, 165–181. [[CrossRef](#)]
9. Berthier, E.; Andrieu, H.; Creutin, J.D. The role of soil in the generation of urban runoff: Development and evaluation of a 2D model. *J. Hydrol.* **2004**, *299*, 252–266. [[CrossRef](#)]
10. Wittenberg, H. Effects of season and man-made changes on baseflow and flow recession: Case studies. *Hydrol. Process.* **2003**, *17*, 2113–2123. [[CrossRef](#)]
11. Thorndahl, S.; Balling, J.D.; Larsen, U.B.B. Analysis and integrated modelling of groundwater infiltration to sewer networks. *Hydrol. Process.* **2016**, *30*, 3228–3238. [[CrossRef](#)]
12. Semadeni-Davies, A.; Hernebring, C.; Svensson, G.; Gustafsson, L.-G. The impacts of climate change and urbanisation on drainage in Helsingborg, Sweden: Combined sewer system. *J. Hydrol.* **2008**, *350*, 100–113. [[CrossRef](#)]
13. Dirckx, G.; Van Daele, S.; Hellinck, N. Groundwater Infiltration Potential (GWIP) as an aid to determining the cause of dilution of waste water. *J. Hydrol.* **2016**, *542*, 474–486. [[CrossRef](#)]
14. Belhadj, N.; Joannis, C.; Raimbault, G. Modelling of rainfall induced infiltration into separate sewerage. *Water Sci. Technol.* **1995**, *32*, 161–168.
15. Dupasquier, B. Modélisation Hydrologique et Hydraulique des Infiltrations D’eaux Parasites dans les Réseaux Séparatifs D’eaux Usées [Hydrological and Hydraulic Modelling of Infiltration into Separate Sanitary Sewers]. Ph.D. Thesis, ENGREF, Paris, France, 26 February 1999.
16. Houhou, J.; Lartiges, B.S.; France-Lanord, C.; Guilmette, C.; Poix, S.; Mustin, C. Isotopic tracing of clear water sources in an urban sewer: A combined water and dissolved sulfate stable isotope approach. *Water Res.* **2010**, *44*, 256–266. [[CrossRef](#)] [[PubMed](#)]
17. De Bondt, K.; Seveno, F.; Petrucci, G.; Rodriguez, F.; Joannis, C.; Claeys, P. Potential and limits of stable isotopes ($\delta^{18}\text{O}$ and δD) to detect parasitic water in sewers of oceanic climate cities. *J. Hydrol. Reg. Stud.* **2018**, *18*, 119–142. [[CrossRef](#)]
18. Beheshti, M.; Saegrov, S. Quantification assessment of extraneous water infiltration and inflow by analysis of the thermal behavior of the sewer network. *Water* **2018**, *10*, 1070. [[CrossRef](#)]
19. Kaushal, S.S.; Belt, K.T. The urban watershed continuum: Evolving spatial and temporal dimensions. *Urban Ecosyst.* **2012**, *15*, 409–435. [[CrossRef](#)]
20. Gessner, M.O.; Hinkelmann, R.; Nützmann, G.; Jekel, M.; Singer, G.; Lewandowski, J.; Nehls, T.; Barjenbruch, M. Urban water interfaces. *J. Hydrol.* **2014**, *514*, 226–232. [[CrossRef](#)]
21. Schlea, D.; Martin, J.F.; Ward, A.D.; Brown, L.C.; Suter, S.A. Performance and water table responses of retrofit rain gardens. *J. Hydrol. Eng.* **2013**, *19*. [[CrossRef](#)]
22. Furumai, H. Rainwater and reclaimed wastewater for sustainable urban water use. *Phys. Chem. Earth* **2008**, *33*, 340–346. [[CrossRef](#)]
23. Roldin, M.; Fryd, O.; Jeppesen, J.; Mark, O.; Binning, P.J.; Mikkelsen, P.S.; Jensen, M.B. Modelling the impact of soakaway retrofits on combined sewage overflows in a 3km² urban catchment in Copenhagen, Denmark. *J. Hydrol.* **2012**, *452*, 64–75. [[CrossRef](#)]
24. Mitchell, V.G.; Mein, R.G.; McMahon, T.A. Modelling the urban water cycle. *Environ. Modell. Softw.* **2001**, *16*, 615–629. [[CrossRef](#)]
25. Rossman, L.A. Storm Water Management Model User’s Manual Version 5.0. U.S. Environmental Protection Agency, EPA/600/R-05/040. 2009. Available online: https://cstdms.colorado.edu/w/images/Epaswmm5_user_manual.pdf (accessed on 24 February 2020).
26. Elliott, A.H.; Trowsdale, S.A. A review of models for low impact urban stormwater drainage. *Environ. Modell. Softw.* **2007**, *22*, 394–405. [[CrossRef](#)]

27. Gustafsson, L.-G. Alternative Drainage Schemes for Reduction of Inflow/Infiltration—Prediction and Follow-Up of Effects with the Aid of an Integrated Sewer/Aquifer Model. 1st International Conference on Urban Drainage via Internet. 2000. Available online: http://www.dhigroup.com/upload/publications/mouse/Gustafsson_Alternative_Drainage.pdf (accessed on 24 February 2020).
28. Wolf, L.; Klinger, J.; Hoetzel, H.; Mohrlök, U. Quantifying mass fluxes from urban drainage systems to the urban soil-aquifer system. *J. Soils Sediments* **2007**, *7*, 85–95. [[CrossRef](#)]
29. Harbaugh, A.W. MODFLOW–2005, the U.S. Geological Survey Modular Ground-Water Model—the Ground-Water Flow Process, Techniques and Methods 6–A16, U.S. Geol. Surv., Reston, Va. 2005. Available online: <https://pubs.er.usgs.gov/publication/tm6A16> (accessed on 24 February 2020).
30. Trefry, M.G.; Muffels, C. FEFLOW: A Finite-Element Ground Water Flow and Transport Modeling Tool. *Ground Water* **2007**, *45*, 525–528. [[CrossRef](#)]
31. Mitchell, V.; Diaper, C.; Gray, S.R.; Rahilly, M. UVQ: Modelling the movement of water and contaminants through the total urban water cycle. In Proceedings of the 28th International Hydrology and Water Resources Symposium: About Water, Wollongong, Australia, 10–13 November 2003. Symposium Proceedings 3.131–3.138.
32. Burn, S.; DeSilva, D.; Ambrose, M.; Meddings, S.; Diaper, C.; Correll, R.; Miller, R.; Wolf, L. A decision support system for urban groundwater resource sustainability. *Water Pract. Technol.* **2006**, *1*, wpt2006010. [[CrossRef](#)]
33. Karpf, C.; Krebs, P. Modelling of groundwater infiltration into sewer systems. *Urban Water J.* **2013**, *10*, 221–229. [[CrossRef](#)]
34. Schirmer, M.; Leschik, S.; Musolff, A. Current research in urban hydrogeology—A review. *Adv. Water Resour.* **2013**, *51*, 280–291. [[CrossRef](#)]
35. Liu, T.; Su, X.; Prigiobbe, V. Groundwater-sewer interaction in urban coastal areas. *Water* **2018**, *10*, 1774. [[CrossRef](#)]
36. Rodriguez, F.; Andrieu, H.; Morena, F. A distributed hydrological model for urbanized areas—Model development and application to case studies. *J. Hydrol.* **2008**, *351*, 268–287. [[CrossRef](#)]
37. Ruban, V.; Rodriguez, F.; Lamprea-Maldonado, K.; Mosini, M.L.; Lebouc, L.; Pichon, P.; Letellier, L.; Rouaud, J.M.; Martinet, L.; Dormal, G.; et al. Le secteur atelier pluridisciplinaire (SAP), un observatoire de l’environnement urbain: Présentation des premiers résultats du suivi hydrologique et microclimatique du bassin du Pin Sec (Nantes). [Interdisciplinary Experimental Observatory dedicated to the urban environment: Presentation of initial hydrological and microclimatic monitoring results from the Pin Sec catchment (Nantes)]. *Bulletin de liaison des Lab. des Ponts et Chaussées* **2010**, *277*, 5–18.
38. BRGM. Notice de la Carte Géologique de Nantes. [Geological Map of Nantes—Instruction] Carte Géologique au 1/50000, Nantes (481). 1970. Available online: <http://infoterre.brgm.fr/page/cartes-geologiques> (accessed on 24 February 2020).
39. Le Delliou, A.-L. Rôle des Interactions Entre les Réseaux D’assainissement et les Eaux Souterraines dans le Fonctionnement Hydrologique D’un Bassin Versant en Milieu Urbanisé—Approche Expérimentale et Modélisations [Sewer Network and Underground Water Interactions Role on the Hydrological Behaviour of an Urban Catchment—Experimental and Modelling Approaches]. Ph.D. Thesis, Ecole Centrale de Nantes (SPIGA), Nantes, France, 7 December 2009. (In French).
40. Hiscock, K. *Hydrogeology: Principles and Practice*; Blackwell Science Ltd.: London UK, 2005.
41. Hvorslev, M.J. Time Lag and Soil Permeability in Ground-Water Observations. Bull. No. 36 1951, Waterways Exper. Sta. Corps of Engrs, U.S. Army, Vicksburg, Mississippi, 1–50. Available online: <https://books.google.com> (accessed on 24 February 2020).
42. Le Delliou, A.L.; Rodriguez, F.; Andrieu, H. Hydrological modelling of sewer network impacts on urban groundwater. *La Houille Blanche* **2009**, *5*, 152–158. [[CrossRef](#)]
43. De Bénédictis, J.; Bertrand-Krajewski, J.-L. Infiltration in sewer systems: Comparison of measurement methods. *Water Sci. Technol.* **2005**, *52*, 219–227. [[CrossRef](#)]
44. Wittenberg, H.; Aksoy, H. Groundwater intrusion into leaky sewer systems. *Water Sci. Technol.* **2010**, *62*, 92–98. [[CrossRef](#)] [[PubMed](#)]
45. Zhang, M.; Liu, Y.; Cheng, X.; Zhu, D.Z.; Shi, H.; Yuan, Z. Quantifying rainfall-derived inflow and infiltration in sanitary sewer systems based on conductivity monitoring. *J. Hydrol.* **2018**, *558*, 174–183. [[CrossRef](#)]

46. Carrera-Hernandez, J.J.; Gaskin, S.J. The groundwater modeling tool for GRASS (GTMG): Open source groundwater flow modeling. *Comput. Geosci.* **2006**, *32*, 339–351. [[CrossRef](#)]
47. Yang, Y.; Lerner, D.N.; Barrett, M.H.; Tellam, J.H. Quantification of groundwater recharge in the city of Nottingham, UK. *Environ. Geol.* **1999**, *38*, 183–198. [[CrossRef](#)]
48. Fatta, D.; Naoum, D.; Loizidou, M. Integrated environmental monitoring and simulation system for use as a management decision support tool in urban areas. *J. Env. Manag.* **2002**, *64*, 333–343. [[CrossRef](#)]
49. Boukhemacha, M.A.; Gogu, C.R.; Serpescu, I.; Gaitanaru, D.; Bica, I. A hydrogeological conceptual approach to study urban groundwater flow in Bucharest city, Romania. *Hydrogeol. J.* **2015**, *23*, 437–450. [[CrossRef](#)]
50. Johnson, A.I. *Specific Yield—Compilation of Specific Yields for Various Materials*; US Geological Survey Water-Supply Paper 1662-D; United States Government Printing Office: Washington, DC, USA, 1967; p. 74.
51. Chiang, W.-H. *3D-Groundwater Modeling with PMWIN: A Simulation System for Modeling Groundwater Flow and Transport Processes*; Springer: Berlin/Heidelberg, Germany, 2005.
52. Cassan, M. *Aide-Mémoire D’hydraulique Souterraine [Groundwater Hydraulic Aide-Memoire]*; Presses de l’Ecole Nationale des Ponts et Chaussées: Paris, France, 1993.
53. Adamiade, V. Influence d’un Fossé sur les Ecoulements Rapides au Sein d’un Versant [The Hydrological Influence of the Ditches on Hillslope Flow: Application to the Pesticides Transfer]. Ph.D. Thesis, Université Pierre et Marie Curie, Géosciences et Ressources Naturelles, Paris, France, 15 March 2004. (In French).
54. Lockmiller, K.A.; Wang, K.; Fike, D.A.; Shaughnessy, A.R.; Hasenmueller, E.A. Using multiple tracers (F-, B, $\delta^{11}\text{B}$, and optical brighteners) to distinguish between municipal drinking water and wastewater inputs to urban streams. *Sci Total Environ* **2019**, *671*, 1245–1256. [[CrossRef](#)]
55. Garcia-Fresca, B.; Sharp, J.-M. Hydrogeologic considerations of urban development: Urban-induced recharge. *Rev. Eng. Geol.* **2005**, *16*, 123–136.
56. Vizintin, G.; Souvent, P.; Veselic, M.; Cencur Curk, B. Determination of urban groundwater pollution in alluvial aquifer using linked process models considering urban water cycle. *J. Hydrol.* **2009**, *377*, 261–273. [[CrossRef](#)]



© 2020 by the authors. Licensee MDPI, Basel, Switzerland. This article is an open access article distributed under the terms and conditions of the Creative Commons Attribution (CC BY) license (<http://creativecommons.org/licenses/by/4.0/>).